Geometrical ambiguity of pair statistics. II. Heterogeneous media

Yang Jiao

Department of Mechanical and Aerospace Engineering, Princeton University, Princeton, New Jersey 08544, USA

Frank H. Stillinger

Department of Chemistry, Princeton University, Princeton, New Jersey 08544, USA

Salvatore Torquato[*]

Department of Chemistry and Department of Physics, Princeton Institute for the Science and Technology of Materials,
Program in Applied and Computational Mathematics, and Princeton Center for Theoretical Science,
Princeton University, Princeton, New Jersey 08544, USA

In the first part of this series of two papers [Y. Jiao, F. H. Stillinger, and S. Torquato, Phys. Rev. E **81**, 011105 (2010)], we considered the geometrical ambiguity of pair statistics associated with point configurations. Here we focus on the analogous problem for heterogeneous media (materials). Heterogeneous media are ubiquitous in a host of contexts, including composites and granular media, biological tissues, ecological patterns, and astrophysical structures. The complex structures of heterogeneous media are usually characterized via statistical descriptors, such as the n-point correlation function S_n. An intricate inverse problem of practical importance is to what extent a medium can be reconstructed from the two-point correlation function S_2 of a target medium. Recently, general claims of the uniqueness of reconstructions using S_2 have been made based on numerical studies, which implies that S_2 suffices to uniquely determine the structure of a medium within certain numerical accuracy. In this paper, we provide a systematic approach to characterize the geometrical ambiguity of S_2 for both continuous two-phase heterogeneous media and their digitized representations in a mathematically precise way. In particular, we derive the exact conditions for the case where two distinct media possess identical S_2, i.e., they form a degenerate pair. The degeneracy conditions are given in terms of integral and algebraic equations for continuous media and their digitized representations, respectively. By examining these equations and constructing their rigorous solutions for specific examples, we conclusively show that in general S_2 is indeed not sufficient information to uniquely determine the structure of the medium, which is consistent with the results of our recent study on heterogeneous-media reconstruction [Y. Jiao, F. H. Stillinger, and S. Torquato, Proc. Natl. Acad. Sci. U.S.A. **106**, 17634 (2009)]. The analytical examples include complex patterns composed of building blocks bearing the letter "T" and the word "WATER" as well as degenerate stacking variants of the densest sphere packing in three dimensions (Barlow films). Several numerical examples of degeneracy (e.g., reconstructions of polycrystal microstructures, laser-speckle patterns and sphere packings) are also given, which are virtually exact solutions of the degeneracy equations. The uniqueness issue of multiphase media reconstructions and additional structural information required to characterize heterogeneous media are discussed, including two-point quantities that contain topological connectedness information about the phases.

I. INTRODUCTION

Two-phase heterogeneous media (textures) abound in nature and synthetic situations. Examples include manufactured heterogeneous materials (e.g., composites, porous media and colloids) [1–4], geologic media (e.g., rock formations) [1,2,5], cellular materials [6], ecological structures (e.g., tree patterns in forests) [7], cosmological structures (e.g., galaxy distributions) [8,9], and biological media (e.g., animal and plant tissue) [10]. In general, the complex microstructures of random media can only be characterized via certain statistical descriptors, such as an infinite set of n-point correlation functions S_n ($n=1,2,\dots$) [1]. It is well known that the effective physical properties of heterogeneous media, such as the

conductivity [11], elastic moduli [12], fluid permeability [13], trapping constant [14] and electromagnetic wave characteristics [15], can be expressed in terms of weighted functionals of S_n. In particular, $S_n(\mathbf{x}_1, \mathbf{x}_2, \dots, \mathbf{x}_n)$ gives the probability of finding n points positioned at $\mathbf{x}_1, \mathbf{x}_2, \dots, \mathbf{x}_n$ all in the phase of interest [1]. For statistically homogeneous media which are the focus of this paper, S_n is translationally invariant and hence depends only on the relative displacements of the positions with respect to some arbitrarily chosen origin, say $\mathbf{x}_1$, i.e., $S_n(\mathbf{x}_1, \mathbf{x}_2, \dots, \mathbf{x}_n) = S_n(\mathbf{x}_{12}, \mathbf{x}_{13}, \dots, \mathbf{x}_{1n})$ with $\mathbf{x}_{ij} = \mathbf{x}_j - \mathbf{x}_i$. In such cases, the one-point correlation function S_1 is just equal to the volume fraction of the phase of interest. If the medium is also statistically isotropic, the two-point correlation function S_2 is a radial function, i.e., $S_2(\mathbf{x}_{12}) = S_2(|\mathbf{x}_{12}|)$, providing information about the distribution of pair-separation distances [16].

*torquato@electron.princeton.edu

Although the S_n can be represented analytically for certain models [1] and bounded for general media [17], it is usually not possible to compute all of the S_n in the infinite set. Thus, it is desirable to understand the extent to which one can characterize the structure and properties of heterogeneous media using lower-order correlation functions, such as the two-point correlation function S_2. A powerful means to study this problem and related questions is to employ inverse techniques [18] whereby one attempts to reconstruct (or construct) realizations of heterogeneous media that match limited structural information of those media in the form of lower-order correlation functions, obtained either experimentally or from theoretical considerations [19,20]. In particular, the reconstruction of digitized representations of heterogeneous materials from a prescribed two-point correlation function S_2 has been receiving considerable attention [21–30]. An effective reconstruction procedure enables one to generate accurate renditions of the medium at will and subsequent analysis can be performed on the reconstruction to obtain desired macroscopic properties of the medium nondestructively.

It has been well established [19,28,31–33] that S_2 is generally devoid of crucial information to uniquely determine the structure of the medium. In particular, in Ref. [33], we employed inverse "reconstruction" techniques to probe the information content of the widest class of different types of two-point functions. This set of functions includes the standard two-point correlation function S_2, surface-void F_{sv} and surface-surface F_{ss} correlation functions [35], lineal-path function L [36], chord-length probability density function p [37], the pore-size function F [1], and the two-point cluster function C_2 [38]. By numerically reconstructing two-phase heterogeneous media from these correlation functions, we unambiguously showed that S_2 does not suffice for a unique reconstruction and that incorporating C_2, which is sensitive to topological connectedness information, can lead to a much more accurate rendition of the target medium. It is worth noting that in most numerical reconstructions, S_2 of the reconstructed medium only matches that of the target medium within certain numerical accuracy [39]. However, it appears that the idea that S_2 is generally devoid of crucial structural information still has not been widely appreciated and claims of uniqueness of reconstructions using S_2 have been made based on numerical studies [22,30]. Thus, our work has implications for the fundamental problem of determining the necessary conditions that realizable two-point functions must possess [40].

In the first part of this series of two papers [34] (henceforth referred to as Part I), we have shown via concrete examples the existence of distinct point configurations possessing identical sets of pair-separation distances. By appropriately decorating the point configurations, distinct two-phase media with identical S_2 can be constructed (see Fig. 1). In general, there are many ways to decorate a point configuration, which enables one to obtain a wide spectrum of distinct heterogeneous media. In this paper, we focus on characterizing the structural ambiguity of pair statistics as embodied in the two-point correlation function S_2 associated with individual realizations of statistically homogeneous two-phase heterogeneous media in a *mathematically precise*
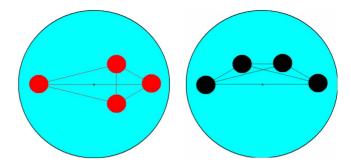

FIG. 1. (Color online) A degenerate pair of two-phase continuous media based on the "kite-trapezoid" example given in Ref. [34]. The longest distance in the "kite" and "trapezoid" is symmetrically placed on the large circle diameter, as adapted from Ref. [34]. Note that this example can be interpreted as two-dimensional (disks) or three-dimensional (spheres).

way, which complements previous numerical studies. In other words, we provide a mathematical formulation for heterogeneous-media reconstructions and rigorously show that distinct media exist that possess exactly identical two-point correlation functions. This objective is quite different from the approximate matching of S_2 that one encounters in numerical simulations, which are also discussed.

The reconstruction of random textures also has a wide spectrum of applications in vision research [32,41,42]. It is important to distinguish a popular two-point statistics used in vision research, called the "dipole histogram," from the two-point correlation function of statistically homogeneous media. The dipole histogram is a particular statistics of the vector pair displacements in a *finite* texture [42]. In such a case, the distinguishable vector pair displacement with the largest length can always be identified together with the positions of the two points that give rise to the displacement. Similarly, one can then identify the second largest displacement and the positions of points possessing this displacement, and so on. Finally, the texture can be completely reconstructed from the dipole histogram. However, we emphasize that this is possible because the information contained in the dipole histogram of a finite texture is not averaged out as that contained in the two-point correlation function of a statistically homogeneous medium. In particular, due to the requirement of translational invariance, periodic boundary conditions are always imposed for realizations of statistically homogeneous media. Thus, only the probabilities of the occurrence of displacements are given by S_2, obtained by averaging over all available positions in the medium, instead of the indication of the actual occurrence of particular displacements at certain positions provided by the dipole histogram. It is such additional information contained in the dipole histogram that enables a unique reconstruction. We will see in the following sections that the position average (i.e., volume average) necessarily leads to the structural ambiguity of S_2.

To provide a quantitative characterization of the structural ambiguity of S_2, we first give the relevant definitions here. Two heterogeneous media are identical if they possess identical sets of n-point correlation functions S_n for $n = 1, 2, \ldots$. Two heterogeneous media are S_k-distinct if they process distinct n-point correlation functions for all $n \geq k$. A heteroge-
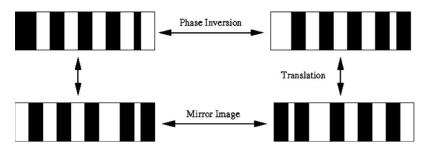
FIG. 2. Illustrations of one-dimensional two-phase random media that form trivial degenerate pairs that we do not count. Note that the arrows indicate that the transformations (e.g., mirror reflection, translation, phase inversion, and these combinations) can occur in either the clockwise or counter-clockwise directions.

neous medium is l-fold degenerate if there exist additional $(l-1)$ media such that all the l media are mutually S_3-distinct but possess the same two-point correlation function S_2. For statistically homogeneous media, the above definition of structural degeneracy rules out the possibility that two degenerate media are trivially connected by a translation, rotation, mirror reflection or any of these combinations (see Fig. 2). This is consistent with our definition of degeneracy for point configuration in the first part of this series two papers [34]. Moreover, we consider that two media do not form a degenerate pair if they possess phase-inversion symmetry at phase volume fractions 0.5, i.e., the morphology of one phase is statistically identical to that of the other phase when the two phases are interchanged [1].

As pointed out in Part I, given pair statistics in the form of S_2 that are associated with degenerate media, it is impossible even in principle to uniquely reconstruct a medium from such S_2. Furthermore, it is important to determine under what conditions the media possess degenerate counterparts. In this paper, we provide a systematic approach to characterize the structural degeneracies associated with the two-point correlation function for both continuous two-phase heterogeneous media and their digitized representations. In particular, we derive the exact conditions for the existence of degeneracy in terms of integral equations for continuous media and algebraic equations for the digitized representations. We show by examining the derived equations that for statistically homogeneous and isotropic media, structural degeneracies generally exist. This explains the long observed nonuniqueness of reconstructions using radial averaged S_2 in many studies [19–21,28,29]. We also provide a variety of concrete examples of degenerate two-phase media, including both analytical constructions and numerical simulations, which respectively are exact and approximate solutions of the degeneracy equations. These examples include analytically constructed patterns composed of building blocks bearing the letter "T" and the word "WATER," degenerate Barlow films (i.e., stacking variants of the densest sphere packing in three dimensions) as well as numerical reconstructions of polycrystal microstructures, laser-speckle patterns, and sphere packings. Moreover, we discuss the degeneracy of multiphase media and additional structural information that can be incorporated to significantly reduce structural degeneracy of heterogeneous media [33].

The rest of the paper is organized as follows: in Sec. II, we introduce the mathematical model of two-phase heterogeneous media and derive the conditions of degeneracy. In Sec. III, we provide the examples of degeneracies for both continuous media and their digitized representations. In Sec. IV, we discuss the degeneracy of multiphase media and ad-

ditional structural information that would be used to reduce degeneracy. In Sec. V, we make concluding remarks.

II. CONDITIONS OF DEGENERACY

In this section, we derive the exact mathematical conditions under which a statistically homogeneous medium possesses degenerate counterparts. For a continuous medium, these conditions take the form of a set of integral equations of the indicator function (defined below) of the phase of interest. For the digitized representations of the medium, which have been extensively investigated in various numerical reconstruction studies, the integral equations reduce to algebraic equations.

A. Continuous media

Consider a statistically homogeneous medium M occupying the region $\mathcal{V}$ in the d-dimensional Euclidean space $\mathbb{R}^d$ ($d=1,2,3$) which is partitioned into two disjoint phases [1]: phase 1, a region $\mathcal{V}_1$ of volume fraction ϕ_1 and phase 2, a region $\mathcal{V}_2$ of volume fraction ϕ_2. It's obvious that $\mathcal{V}_1 \cup \mathcal{V}_2 = \mathcal{V}$ and $\mathcal{V}_1 \cap \mathcal{V}_2 = \mathbf{0}$. The indicator function $\mathcal{I}^{(i)}(\mathbf{x})$ of phase i is given by

$$\mathcal{I}^{(i)}(\mathbf{x}) = \begin{cases} 1 & \mathbf{x} \in \mathcal{V}_i, \\ 0 & \mathbf{x} \in \overline{\mathcal{V}}_i, \end{cases} \tag{1}$$

for $i=1,2$ with $\mathcal{V}_i \cup \overline{\mathcal{V}}_i = \mathcal{V}$ and

$$\mathcal{I}^{(1)}(\mathbf{x}) + \mathcal{I}^{(2)}(\mathbf{x}) = 1. \tag{2}$$

The n-point correlation function $S_n^{(i)}$ for phase i is defined as follows:

$$S_n^{(i)}(\mathbf{x}_1, \mathbf{x}_2, \ldots, \mathbf{x}_n,) = \langle \mathcal{I}^{(i)}(\mathbf{x}_1) \mathcal{I}^{(i)}(\mathbf{x}_2) \ldots \mathcal{I}^{(i)}(\mathbf{x}_n) \rangle, \tag{3}$$

where the angular brackets "$\langle \ldots \rangle$" denote ensemble averaging over independent realizations of the medium. The two-point correlation function $S_2^{(i)}$ for phase i is defined by

$$S_2^{(i)}(\mathbf{x}_1, \mathbf{x}_2) = \langle \mathcal{I}^{(i)}(\mathbf{x}_1) \mathcal{I}^{(i)}(\mathbf{x}_2) \rangle. \tag{4}$$

As pointed out in Sec. I, for a statistically homogeneous medium, $S_2^{(i)}$ is a function of the relative displacements of point pairs, i.e.,

$$S_2^{(i)}(\mathbf{x}_1, \mathbf{x}_2) = S_2^{(i)}(\mathbf{x}_2 - \mathbf{x}_1) = S_2^{(i)}(\mathbf{r}), \tag{5}$$

where $\mathbf{r} = \mathbf{x}_2 - \mathbf{x}_1$. In the infinite volume limit, if the medium is also ergodic the ensemble average is equivalent to the volume average, i.e.,

$$S_2^{(i)}(\mathbf{r}) = \lim_{V \to \infty} \frac{1}{V} \int_V \mathcal{I}^{(i)}(\mathbf{x}) \mathcal{I}^{(i)}(\mathbf{x} + \mathbf{r}) d\mathbf{x}. \tag{6}$$

If the medium is also statistically isotropic, $S_2^{(i)}$ is a radial function, depending on the separation distances of point pairs only, i.e.,

$$S_2^{(i)}(\mathbf{x}_1, \mathbf{x}_2) = S_2^{(i)}(|\mathbf{r}|) = S_2^{(i)}(r). \tag{7}$$

Readers are referred to Ref. [1] for a detailed discussion of $S_2^{(i)}$ and other higher order $S_n^{(i)}$. Henceforth, we will drop the superscript i in $S_2^{(i)}$ for simplicity. Without further elaboration, S_2 is always the two-point correlation function of the phase of interest.

Now consider a change in the geometry of the region of the phase of interest, say phase 1, that keeps the volume fraction ϕ_1 invariant. The medium after the change is denoted by M' and recall that the original medium is denoted by M. The indicator function $\mathcal{I}'$ of phase 1 in M' is then given by

$$\mathcal{I}'(\mathbf{x}) = \begin{cases} 1 & \mathbf{x} \in \mathcal{V}_1', \\ 0 & \mathbf{x} \in \overline{\mathcal{V}_1'}, \end{cases} \tag{8}$$

where $\mathcal{V}_1'$ is the region where phase 1 is found in M'. We define the change of indicator function as

$$\delta\mathcal{I}(\mathbf{x}) = \mathcal{I}'(\mathbf{x}) - \mathcal{I}(\mathbf{x}), \tag{9}$$

where $\mathcal{I}$ is the indicator function of phase 1 in M given by Eq. (1) with $i=1$. It is obviously that $\delta\mathcal{I}$ can only take the value of 0, −1, and 1. And the requirement that M and M' form a degenerate pair with the same two-point correlation function as well as the same phase volume fractions will lead to constraining equations on $\delta\mathcal{I}$, which are the degeneracy conditions we are seeking.

For simplicity, we introduce a short notation for the integral in Eq. (6), i.e.,

$$S_2 = \frac{1}{V} \mathcal{I} \otimes \mathcal{I}. \tag{10}$$

The requirement that S_2 is invariant under the change δI leads to

$$S_2' = S_2 = \frac{1}{V} \mathcal{I}' \otimes \mathcal{I}' = \frac{1}{V} \mathcal{I} \otimes \mathcal{I}, \tag{11}$$

Substituting Eq. (9) into Eq. (11) yields

$$\frac{1}{V}(\mathcal{I} + \delta\mathcal{I}) \otimes (\mathcal{I} + \delta\mathcal{I}) = \frac{1}{V} \mathcal{I} \otimes \mathcal{I}. \tag{12}$$

From Eq. (12) we can obtain that

$$\left(\mathcal{I} + \frac{1}{2}\delta\mathcal{I}\right) \otimes \delta\mathcal{I} + \delta\mathcal{I} \otimes \left(\mathcal{I} + \frac{1}{2}\delta\mathcal{I}\right) = 0. \tag{13}$$

Note that given the indicator function $\mathcal{I}$ of the original medium M, Eq. (13) should be satisfied by $\delta\mathcal{I}$ for all $\mathbf{r}$ within the range of interest. In other words, Eq. (13) specifies a continuous spectrum of equations, one for each $\delta\mathcal{I}$ at a

particular $\mathbf{r}$. Another requirement for degeneracy is that the phase volume fractions are conserved, which leads to

$$\frac{1}{V} \int_V \mathcal{I}'(\mathbf{x}) d\mathbf{x} = \frac{1}{V} \int_V \mathcal{I}(\mathbf{x}) d\mathbf{x}. \tag{14}$$

Substituting Eqs. (9) into Eq. (14), we can obtain that

$$\int_V \delta\mathcal{I}(\mathbf{x}) d\mathbf{x} = 0. \tag{15}$$

If the medium M is also statistically isotropic, S_2 depends only on pair-separation distances, i.e.,

$$S_2(r) = \frac{1}{\Omega} \int_\Theta S_2(\mathbf{r}) d\Theta, \tag{16}$$

where the integral over d-dimensional solid angle Θ is to average over all directions of $\mathbf{r}$ with the same length r and Ω is the total solid angle. Thus from Eq. (13), we obtain that

$$\int_\Theta \left[\left(\mathcal{I} + \frac{1}{2}\delta\mathcal{I} \right) \otimes \delta\mathcal{I} + \delta\mathcal{I} \otimes \left(\mathcal{I} + \frac{1}{2}\delta\mathcal{I} \right) \right] d\Theta = 0. \tag{17}$$

Note that Eq. (17) should be satisfied by $\delta\mathcal{I}$ for all r within the range of interest.

Thus, it is clear that for the statistically homogeneous medium M, its structural degeneracy M' exists only if Eqs. (13) and (15) possess nontrivial solutions; and the degeneracy exists only if Eqs. (17) and (15) possess nontrivial solutions if M is also statistically isotropic. In principle, from the solutions of Eqs. (13) [or Eq. (17)] and Eq. (15) together with the indicator function $\mathcal{I}$ of the original medium, one can obtain the indicator function $\mathcal{I}'$ of the degenerate medium by applying Eq. (9). Henceforth, we will call Eq. (15) the *feasibility* condition, since it requires that δI must be feasible in the sense that the phase volume fractions are conserved. Similarly, we will call Eqs. (13) and (17) the *invariance* condition, since they give a set of $\delta\mathcal{I}$ that leave S_2 invariant under the change.

B. Digitized media

For a digitized medium M in $\mathbb{R}^d$, the indicator function takes the form of a finite d-dimensional array $\mathbf{I} = [I_{x_1 \ldots x_d}]$ of linear size N, where $I_{x_1 \ldots x_d} = 0$ or 1 indicating the phase of the pixel at $(x_1 \ldots x_d)$ and $x_i = 1, \ldots, N$ for $i = 1, \ldots, d$. Consider a perturbation of the geometry of phase 1 in the digitized medium M that preserves the phase volume fractions (e.g., by exchanging pixels of different phases). The perturbed medium with the indicator function $\mathbf{I}' = [I'_{x_1 \ldots x_d}]$ is denoted by M'. The change of the indicator function is simply

$$\delta\mathbf{I} = \mathbf{I}' - \mathbf{I} = [I'_{x_1 \ldots x_d} - I_{x_1 \ldots x_d}] = [\delta I_{x_1 \ldots x_d}], \tag{18}$$

which is also a d-dimensional matrix with linear size N. The entries $\delta I_{x_1 \ldots x_d}$ can only take the values −1, 0, and 1.

For statistically homogeneous digitized media, periodic boundary conditions are imposed by the requirement of

translational invariance. Thus, the indices of the indicator functions are modulated by N, i.e., if $(x_i+r_i) \geq N$ the index should take the value (x_i+r_i-N) instead, where x_i is the original index and r_i is the translation displacement along x_i direction. On the other hand, if $(x_i+r_i) < 0$ the index should take the value (x_i+r_i+N) instead. The integral equations of the feasibility condition (15) reduce to algebraic equations, i.e.,

$$\sum_{x_1,\ldots,x_d} \delta I_{x_1\ldots x_d} = 0, \tag{19}$$

where the sum is running through $x_i=1,\ldots,N$ for $i=1,\ldots,d$. The equations for the invariance condition reduce to

$$\sum_{(x_1,\ldots,x_d)\in H_1} \delta I_{x_1\ldots x_d} + \sum_{(x_1,\ldots,x_d)\in H_2} \delta I_{(x_1+r_1)\ldots(x_d+r_d)}$$
$$+ \sum_{x_1,\ldots,x_d} \delta I_{x_1\ldots x_d} \delta I_{(x_1+r_1)\ldots(x_d+r_d)} = 0, \tag{20}$$

where r_i $(i=1,\ldots,d)$ are integers satisfying $|r_i| \leq N/2$ and the sets of pixel positions H_1 and H_2 are given by

$$H_1 = \{(x_1,\ldots,x_d) | I_{(x_1+r_1)\ldots(x_d+r_d)} = 1\},$$

$$H_2 = \{(x_1,\ldots,x_d) | I_{x_1\ldots x_d} = 1\}. \tag{21}$$

If the medium is also statistically isotropic, following Eq. (17) the invariance conditions can be obtained by averaging Eq. (20) over equivalent directions, i.e.,

$$\sum_{(r_1,\ldots,r_d)\in\Omega} \left(\sum_{(x_1,\ldots,x_d)\in H_1} \delta I_{x_1\ldots x_d} + \sum_{(x_1,\ldots,x_d)\in H_2} \delta I_{(x_1+r_1)\ldots(x_d+r_d)} \right.$$
$$\left. + \sum_{x_1,\ldots,x_d} \delta I_{x_1\ldots x_d} \delta I_{(x_1+r_1)\ldots(x_d+r_d)} \right) = 0, \tag{22}$$

where the sets of displacements with the same length Ω and the sets of pixel positions H_1 and H_2 are given by

$$\Omega = \{(r_1,\ldots,r_d) | r_1^2 + \cdots + r_d^2 = r^2,\ r \in \mathbb{Z},\ r \leq N/2\},$$

$$H_1 = \{(r_1,\ldots,r_d) | I_{(x_1+r_1)\ldots(x_d+r_d)} = 1\},$$

$$H_2 = \{(r_1,\ldots,r_d) | I_{x_1\ldots x_d} = 1\}. \tag{23}$$

Thus, similar to their continuous counterparts, two statistically homogeneous digitized media M and M' form a degenerate pair if the feasibility condition Eq. (19) and the invariance condition Eq. (20) hold for some nontrivial $\delta\mathbf{I}$. If the media are also statistically isotropic, the degeneracy exists if Eqs. (19) and (22) possess nontrivial solutions. Once $\delta\mathbf{I}$ is obtained, the degenerate medium M' can be constructed by applying Eq. (18).

Note that in Eq. (22), because the number of equations (i.e., the total number of integers that are smaller than $N^2/4$) is in general much smaller than the number of unknowns (i.e., the number of the entries $I_{x_1\ldots x_d}$ which is equal to N^d), the algebraic Eqs. (22) possess multiple solutions. For such isotropic media, it is highly probable to obtain degeneracies of the original medium in a reconstruction. This explains the
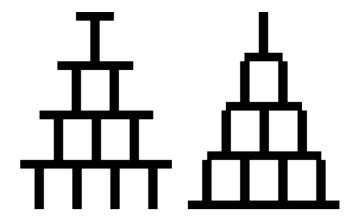

FIG. 3. A simple degeneracy example composed of replications of letter "T."

long observed nonuniqueness issue in the reconstruction of heterogeneous media using radial S_2 [19,20,28,29]. The situation is more subtle for general statistically homogeneous media, for which the degeneracy condition Eq. (20) contains the same number of equations and unknowns. Thus, the chances for finding a nontrivial solution of $\delta\mathbf{I}$ is much smaller but one still cannot rule out the possibility of degeneracy. It is clear that the solutions also depend on the original medium, i.e., the values of $I_{x_1\ldots x_d}$. In the following section, we will show the existence of degeneracies for both continuous and digitized media via concrete examples, which are solutions of the above degeneracy equations.

III. EXAMPLES OF DEGENERACY

In this section, we will provide concrete examples of structural degeneracy. These examples include both exact and approximate solutions of the equations for degeneracy derived in the previous section. For continuous and simple digitized media, analytical constructions are given. For more complicated digitized media, numerical simulations are employed to find degeneracies. For a clear illustration, we will mainly focus on two-dimensional examples here. However, the general construction methods can be also applied to find degenerate media in any space dimension.

A. Analytical constructions

1. Vector-argument $S_2(\mathbf{r})$

As discussed in Sec. II A, the two-point correlation function $S_2(\mathbf{r})$ contains information on the relative displacements (vector distances) between any two points in the phase of interest. Consider a two-phase medium, in which one of the phases is composed of replications of certain substructures. If the substructures do not possess central inversion symmetry, they can be rotated in a way such that all the relative displacements of point pairs within and among the substructures remain the same yet the overall structure (the replication of the rotated substructures) is different from the original one. A simple example originally proposed in Ref. [41] is shown in Fig. 3. The substructure, i.e., the letter "T," has been arranged into a "pyramid." By rotating each "T" about
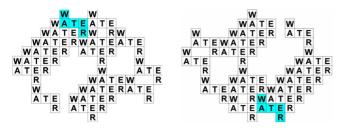
FIG. 4. (Color online) A more sophisticated degeneracy example composed of replications of the letters "WATER." One "S"-shaped auxiliary box is shown in blue (or light gray in the print version).

an axis perpendicular to the plane by 180°, a distinct structure can be produced. Since the relative orientation of the position of any pair of letters "T" has not changed, the relative displacements of the point pairs, one from each of different "T" also remain the same. It is obvious that the relative displacements of point pairs within any single "T" are not affected. Thus, the two distinct structures possess identical statistics of relative displacements of point pairs, i.e., identical two-point correlation functions $S_2(\mathbf{r})$, so they form a degenerate pair.

Figure 4 shows a more sophisticated example based on the same construction rule. The substructure now is composed of the letters "WATER" arranged in an "S"-shaped auxiliary box (shown in blue or light gray in print version), which is then replicated in a complicated way. Note that though the auxiliary box possesses central inversion symmetry, the substructure composed of the letters does not. By rotating each substructure about the inversion symmetry axis of the corresponding auxiliary box, a degenerate structure can be constructed. Note these examples are exact solutions of the Eqs. (15) and (13).

2. Radially averaged $S_2(r)$

Radially averaged $S_2(r)$ only contains information on separation distances between the point pairs in the phase of interest. In the best case, the complete set of pair-separation distances can be inferred from $S_2(r)$. Such distance sets have been studied in detail in Part I of this series of two papers, where we have shown that a variety of classes of degeneracies can be identified that are compatible with the given distance set of a point configuration. In particular, we pointed out in Part I that by decorating the degenerate point configurations properly, degenerate two-phase media can be constructed. One such example is to decorate the 30 degenerate tetrahedra discussed in Part I, e.g., one can place the centroids of congruent spheres at the vertices of the tetrahedra and choose the "sphere" phase as the phase of interest and the space exterior to spheres as "void" phase. Then the 30 heterogeneous media associated these tetrahedra are degenerate.

Another example constructed by decorating a point configuration is shown in Fig. 5, where the two circular-disk packings form a degenerate pair. The packings contain three types of particles: a large number of the circular disks (shown in black) form a cluster with central symmetry. Three particles (shown in blue) arranged on a straight line form a
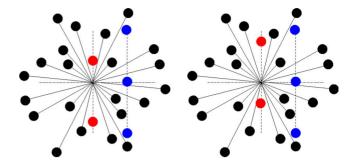

FIG. 5. (Color online) A degenerate pair of circular-disk packings in two dimensions.

substructure possessing mirror reflection symmetry, i.e., the two most separated particles are located symmetrically about the one in the middle. The remaining two (shown in red) are placed along a line parallel to that of the three blue particles and going through the center of the symmetric cluster, such that the set of relative distances between any two points in the "particle" phase in the two packings are identical while the two resulting structures are distinct. The constructed degenerate pair is an exact solution of the Eqs. (15) and (17).

Note that the aforementioned degeneracy construction rules are also applicable in the case of digitized media. For example, applying the construction rule for the degenerate circular-disk packings in Fig. 5 to a two-dimensional square lattice of pixels results in the degenerate digitized media shown in Fig. 6. The only difference is an additional requirement that for digitized media the values of the distances must be square roots of integers and the symmetry groups of the structures are discrete, which reduces the total number of possible degeneracies.

3. Degenerate Barlow films

Another class of interesting degeneracy examples associated with radially averaged S_2 involves the Barlow packings, i.e., random stackings of infinite triangular-lattice layers of spheres. In a Barlow packing, for a particular layer (i.e., layer "A") there are only two possible positions for the next layer, which we denote by the usual code as "B" and "C," respectively. Thus, a Barlow packing can be represented by a sequence of "A," "B," and "C," e.g., "…ABCBCA…." A Barlow film is a Barlow packing consisting of a finite number of layers. The distribution of pair distances in such a
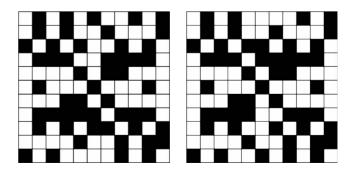

FIG. 6. A degenerate pair of digitized media based on the same construction rules for the degenerate circular-disk packings.

TABLE I. The number of the same species ("AA," "BB," or "CC") at different layer-separation distances for the six-layer degenerate Barlow pair "ABABAC" and "ABABCB." d_L is the layer-separation distance.

d_L	"ABABAC"	"ABABCB"
1	0	0
2	3	3
3	0	0
4	1	1
5	0	0

TABLE II. The number of degenerate Barlow film configurations for $n \in [6, 15]$. n is the number of layers in the Barlow film. N_{pair} is the number of degenerate pairs and $N_{triplet}$ is the number of degenerate triplets.

Number of layers	N_{pair}	$N_{triplet}$
$n=6$	1	0
$n=7$	1	0
$n=8$	5	0
$n=9$	4	0
$n=10$	16	1
$n=11$	13	0
$n=12$	54	6
$n=13$	35	2
$n=14$	157	13
$n=15$	123	5

geometry depends not only on how many layers are present, but also upon whether any chosen pair of layers is the same species ("AA," "BB," or "CC"), or different species ("AB," "AC," or "BC"). This motivates counting "same" versus "different" species for each separation distance between layer pairs. The distance distribution (i.e., S_2) is completely determined by the number of same species at all separation distances between layer pairs.

For an n-layer Barlow film, there are nominally 2^n possible configurations. However, not all of these 2^n configurations are distinct. A basic property of Barlow films is that the distance distribution is invariant under a "renaming" operation. For example, the sequences "ABCABC," "BCABCA," and "CABCAB" possess the same structure. In light of this "renaming" invariance, we can require that the first two layers for all Barlow films to be "AB..." without loss of generality. Thus, the number of distinct configurations associated with an n-layer Barlow film that possess the same vertical distances between identical layers (i.e., the same distance distributions) is reduced to $2^{(n-2)}$. As mentioned in Sec. I, reflection (mirror image) symmetry should also be excluded for degenerate pairs.

We then set out to identify degenerate Barlow film configurations up to $n=15$ layers by explicitly generating all Barlow films and compare their layer-separation distance distributions. For $n<6$, there are no degenerate configurations. An interesting case occurs at $n=6$, with an inequivalent pair of Barlow films that have the same distance distribution, and thus the same S_2 associated with the "sphere" phase. They can be represented by "ABABAC" and "ABABCB." As shown in Table I, the two configurations possess the same number of same layer species at all layer-separation distances. In addition, they are not related by "renaming" and/or reflection operations.

The numbers of degenerate configurations for $n \in [6, 15]$ are given in Table II. We note that the first degenerate triplet occurs at $n=10$, which includes the configurations "ABABCBACAC," "ABABCBCBAC," and "ABACBCBCAC." We don't find any fourfold degenerate Barlow films for the n values we examined. It can be seen from the table that except for the trivial cases with $n=6$ and 7 the numbers of degeneracies possess the following trends: (i) for both the even-layer and the odd-layer films, the number and complexity of degeneracies increase monotonically as the number of layers increases; (ii) the number of degeneracies associated with an even layer is larger than that of the next odd layer. The latter

trend is probably due to the odd layers having relatively fewer degrees of freedom to exclude the "renaming" and reflection symmetry.

It is also worth noting that if a honeycomb crystal packing of spheres are used for the layers instead of triangular-lattice packings, one can construct degenerate low-density jammed sphere packings [43]. In particular, a honeycomb crystal layer can be obtained by removing one third of the spheres from the triangular-lattice layer. These removed spheres are also arranged on a triangular lattice, but with lattice vectors that are twice in magnitude of those of the original triangular lattice. To obtain honeycomb crystal films from two degenerate Barlow films, exactly the same pair distances are removed associated with the removing of the spheres. Thus, the two constructed honeycomb crystal films also form a degenerate pair. So far, we have not found any degeneracy in the periodic Barlow films.

B. Numerical examples

In many practical applications, one encounters the issue of reconstructing the structures of materials from radially averaged two-point function $S_2(r)$, which might be the only available information at hand and it is always associated with an inevitable uncertainty. Therefore, it is also important to explore the structural degeneracy of $S_2(r)$ subject to small uncertainties. In this section, we employ the Yeong-Torquato heterogeneous material reconstruction procedure [19,20] to obtain numerical-degeneracy examples of statistically homogeneous and isotropic media, which are approximate solutions of the invariance Eqs. (22) derived in Sec. II B. In particular, the "energy" or *mean squared error E* for the reconstruction problem which has been defined previously [19,20,28,29,33] is given by

$$E = \sum_r [\hat{S}_2(r) - S_2(r)]^2, \qquad (24)$$

where $\hat{S}_2$ and S_2 are the target and the reconstructed correlation functions, respectively. In the Yeong-Torquato proce-

(a)
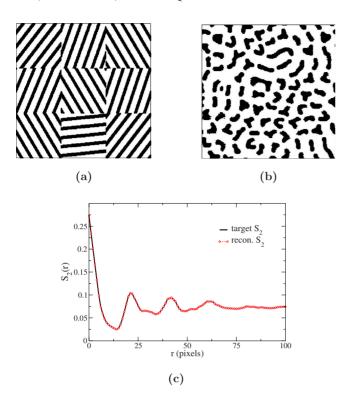

(b)

(a)

(b)

(c)

(c)

FIG. 7. (Color online) The "polycrystal" microstructures. (a) The target medium, in which the volume fraction of the black phase is 0.273. (b) The reconstructed medium using the Yeong-Torquato procedure [19]. (c) The two-point correlation functions of the target and reconstructed media. The mean squared error E defined by Eq. (24) is on the order of 10^{-7}.
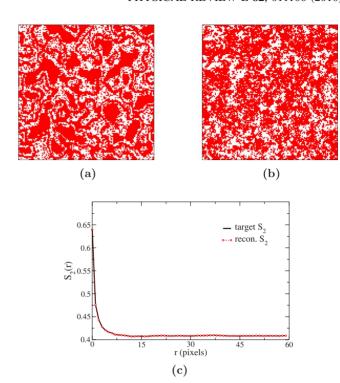
FIG. 8. (Color online) The laser-speckle patterns. (a) The target medium, in which the volume fraction of the red phase is 0.639. (b) The reconstructed medium using the Yeong-Torquato procedure [19]. (c) The two-point correlation functions for the red phase of the target and reconstructed media. The mean squared error E defined by Eq. (24) is on the order of 10^{-7}.

dure, a stochastic optimization technique is used to make E in principle zero. However, in practice E is always a very small number, which corresponds to the situation where the uncertainty associated with S_2 is very small.

We first consider an idealized microstructure of a two-dimensional "polycrystal" shown in Fig. 7(a). The "polycrystal" contains nine square "grains," each associated with a particular orientation as determined by the direction of the black "stripes." The two-point correlation function of the black phase is shown in Fig. 7(c). It can be seen that the oscillations of S_2 are the clear manifestation of the strong spatial correlations between the "stripes." The reconstructed structure is shown in Fig. 7(b), whose S_2 closely matches the target one with a very small error, i.e., sum of squared difference between the two, on the order of 10^{-7}. Though several stripelike substructures have been roughly reproduced and a few weakly preferred orientations of the substructures can be identified, the reconstruction is distinctly different from the target structure in that it contains much more compact substructures and the grain boundaries are completely missing. The correlations due to the alternating "stripes" in the target medium are mimicked by the correlations between the compact substructures with interspaces that are approximately equal to those between the "stripes."

Another interesting example is the reconstruction of a laser-speckle pattern, which contains various shaped substructures on a broad range of length scales [29] [see Fig. 8(a)]. The two-point correlation function [shown in Fig. 8(c)]

clearly does not reflect the multiscale nature of speckle pattern, which monotonically decreases to its long range value very fast. The reconstructed pattern is shown in Fig. 8(b), with a small error between the correlation function on the order of 10^{-7}. The substructures on different length scales in the target medium (e.g., the disconnected compact clusters, stripelike structures and individual pixels) are all mixed up in the reconstruction (e.g., the percolated clusters with different sizes and shapes) to reproduce the short-ranged correlations conveyed in S_2. The reconstructed pattern mimics that of the Debye random medium, a famous model structure containing "clusters of all sizes and shapes" with a exponential two-point correlation function [1,19].

The above two example clearly show that $S_2(r)$ is not able to resolve the details of the substructures in a complex medium. But even for simpler structures, $S_2(r)$ may still be insufficient. Consider a realization of a three-dimensional equilibrium hard-sphere packing [33] [see Fig. 9(a)], generated via standard Monte Carlo simulations. The volume fraction of the sphere phase is close to the percolation threshold. The reconstruction is shown in Fig. 9(b), in which the "sphere" phase forms a complex percolating structure. The error between the target and reconstructed $S_2(r)$ is on the order of 10^{-11}. It is clear that S_2 grossly overestimates the percolation of the target phases, which is due to its insensitivity to the topological connectedness information of the media. This insufficiency of S_2 has was pointed out previously [19,20].

Note that in the above examples, there are small but nonzero errors between the target and reconstructed $S_2(r)$. This
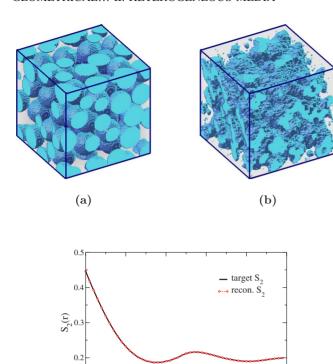
(a)   (b)

(c)

FIG. 9. (Color online) The hard-sphere packings. (a) The target medium, in which the volume fraction of the sphere (blue) phase is 0.446. (b) The reconstructed medium using the Yeong-Torquato procedure [19]. (c) The two-point correlation functions of the target and reconstructed media. The mean squared error E defined by Eq. (24) is on the order of 10^{-11}.

is an algorithmic implementation issue and can be removed if one used integers instead of floating point numbers in the computer program. However, in real-world applications, the obtained $S_2(r)$ data would in general suffer small but finite errors, no matter how carefully the measuring experiments might be carried out. These examples clearly reveal the insufficiency of S_2 in characterizing multiscale structures and those near percolation. Possible candidate correlation functions to overcome these shortcomings are discussed in Sec. IV B. The examples given here are also approximate solutions of the invariance Eqs. (22) derived in Sec. II B.

IV. DISCUSSION

A. Generalization to multiphase media

It is worth noting that although the focus of this paper is two-phase heterogeneous media, it is straightforward to generalize the discussion to multiphase media. In particular, consider a medium composed of p distinct phases, each associated with an indicator function $\mathcal{I}^{(i)}(\mathbf{x})$ ($i=1,\ldots,p$) which equals unity when $\mathbf{x}$ falls in phase i and equals to zero otherwise. There are in total p^2 two-point correlation functions $S_2^{(ij)}(\mathbf{r})$ including p autocorrelations (i.e., when $i=j$ and the two points separated by displacement $\mathbf{r}$ falling into the same

phase) and (p^2-p) cross-correlations (i.e., when $i \neq j$ and the two points falling into different phases i and j). However, there are only $p(p-1)/2$ independent correlation functions since the p indicator functions satisfy the equation

$$\mathcal{I}^{(1)}(\mathbf{x}) + \mathcal{I}^{(2)}(\mathbf{x}) + \cdots + \mathcal{I}^{(p)}(\mathbf{x}) = 1, \qquad (25)$$

and thus, there are only $(p-1)$ independent $\mathcal{I}^{(i)}$.

For every one of the $p(p-1)/2$ independent two-point correlation functions, similar feasibility and invariance conditions can be derived, which take the form of integral or algebraic equations of the variations of the indicator functions for the corresponding phases, as those derived in Sec. II. We will not provide the details of such derivations here. In addition, the same arguments concerning the nonuniqueness of the solutions apply in the case of multiphase media, and thus one cannot rule out the possibility of structural degeneracy.

Two simple examples of degenerate three-phase media are shown in Figs. 10 and 11, which are constructed based on the circular-disk packings and their digitized analog given in Sec. IV A, respectively. A subset of the particles (pixels) have been assigned to the third phase, while all the pair-separation distances in the media remain the same. Thus, any pair of independent two-point correlation functions of the two degenerate media are identical.

B. Additional structural information

By examining the degeneracy conditions and constructing concrete examples, we have established that two-point cor-
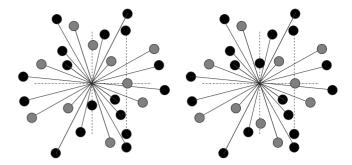

FIG. 10. A degenerate pair of continuous three-phase media (black, white, and gray) constructed based on the degenerate circular-disk packings shown in Fig. 5.
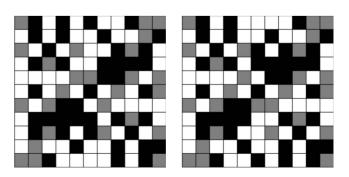

FIG. 11. A degenerate pair of digitized three-phase media (black, white and gray) constructed based on the degenerate media show in Fig. 6.
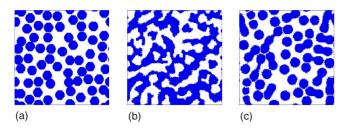
FIG. 12. (Color online) A circular-disk system containing small clusters. (a) Target medium, the volume fraction of the "disk" (blue) phase is 0.532. (b) Reconstruction using S_2 alone. (c) Reconstruction incorporating both S_2 and C_2.

relation function is in general not sufficient to uniquely determine the structure of a heterogeneous medium and degenerate structures do exist, especially for statistically homogeneous and isotropic media. A natural question is what additional structural information could be used to reduce the degeneracy.

It is notoriously difficult to find the complete answer to the above question. However, we have shown in Ref. [33] that it would be a fruitful approach to seek the most sensitive statistical descriptors among the various two-point correlation functions (e.g., the surface functions and cluster-type functions [1]) instead of using standard higher-order n-point correlation functions, as such S_3. The two-point quantities are superior to S_3 in that their determination requires less effort and they are sensitive to nontrivial structural information that is not explicitly contained in S_3, such as the topologically connectedness information.

In particular, a superior descriptor proposed in Ref. [33] is the two-point cluster function $C_2(\mathbf{r})$, which gives the probability of finding two points separated by $\mathbf{r}$ falling in the same cluster of the phase of interest. A reconstruction example of a two-dimensional circular-disk system containing small clusters from both S_2 and C_2 are shown in Fig. 12. It can be seen clearly that S_2-alone reconstruction grossly overestimates the percolation of the "disk" phase, while the reconstruction incorporating C_2 successfully reproduces the disks with small clusters.

We note that proper clustering information can also be used to distinguish certain degeneracy examples provided in this paper. Consider the degenerate media bearing a "kite" and "trapezoid" structure, respectively, shown in Fig. 1, which are obtained by decorating corresponding degenerate point configurations. If we increase the size of the circular disks while keeping their centers fixed, there exists a critical disk diameter at which the three disks in the medium bearing the "kite" structure form a connected "triangle," which is separated from the remaining disk; while in the medium bearing the "trapezoid" structure all the disks belong to a single linear cluster. Because the connected "triangle" of disks only exists in the medium bearing the "kite" structure, the degenerate pair now can be distinguished, i.e., the degeneracy is reduced by using the connectedness (i.e., clustering)

information. It is clear that in this case the clustering information reflects nontrivial triangle information in the system, which is contained in S_3.

V. CONCLUDING REMARKS

In this paper, we discussed various aspects of the structural degeneracy associated with the two-point correlation function S_2 of heterogeneous media. Complementary to previous studies, here we provide precise mathematical formulations for structural degeneracy and rigorously show that distinct media with exactly identical S_2 do exist. In particular, we derived the exact conditions for the existence of degeneracy in terms of integral equations for continuous media and algebraic equations for their digitized representations. By examining the equations and constructing their solutions for specific examples, we have well established that in general S_2 is not sufficient to uniquely determine the structures of the media, contrary to previous claims of the uniqueness of S_2-reconstructions based on numerical studies. We have also provided a variety of concrete examples of degenerate two-phase media, including both analytical constructions and numerical simulations, which are, respectively, exact and approximate solutions of the degeneracy equations. These examples include analytically constructed patterns composed of building blocks bearing the letter "T" and the word "WATER," degenerate Barlow films as well as numerical reconstructions of polycrystal microstructures, laser-speckle patterns and sphere packings. It is clearly seen from these examples that S_2 alone is unable to resolve the details of the microstructures and usually overestimates the percolation in the media, which is consistent with the results of our recent study on the reconstruction of heterogeneous media using a wide spectrum of statistical microstructure descriptors including S_2 [33]. The conclusions also apply in the case of multiphase media.

We have pointed out that it is necessary to include additional information to better characterize the structure of complex heterogeneous media beyond that contained in S_2. In Sec. IV B and Ref. [33], we have shown that the two-point cluster function C_2 (i.e., topologically connectedness information) is a superior microstructure descriptor for media containing compact clusters and its incorporation can significant reduce the degeneracy. For more complex media such as those contain multiscale substructures, structural degeneracy associated with higher order S_n would exist, for example, we may find media that possess distinct $S_4, S_5, \ldots$ but identical S_2 and S_3. In future work, we will focus on identifying such higher-order degeneracies and seeking efficient statistical descriptors (e.g., higher-order versions of C_2) that can capture the salient features of such media.

ACKNOWLEDGMENTS

[1] S. Torquato, *Random Heterogeneous Materials: Microstructure and Macroscopic Properties* (Springer-Verlag, New York, 2002).

[2] M. Sahimi, *Heterogeneous Materials* (Springer-Verlag, New York, 2003).

[3] T. I. Zohdi, Mech. Mater. **38**, 969 (2006).

[4] A. Mejdoubi and C. Brosseau, J. Appl. Phys. **101**, 084109 (2007).

[5] D. A. Coker, S. Torquato, and J. Dunsmuir, J. Geophys. Res. **101**, 17497 (1996).

[6] L. J. Gibson and M. F. Ashby, *Cellular Solids* (Cambridge University Press, Cambridge, England, 1999).

[7] A. Pommerening and D. Stoyan, Can. J. For. Res. **38**, 1110 (2008).

[8] P. J. E. Peebles, *Principles of Physical Cosmology* (Princeton University Press, Princeton, NJ, 1993).

[9] A. Gabrielli, F. Sylos Labini, M. Joyce, and P. Pietronero, *Statistical Physics for Cosmic Structures* (Springer-Verlag, New York, 2005).

[10] A. R. Kherlopian, T. Song, Q. Duan, M. A. Neimark, M. J. Po, J. K. Gohagan, and A. F. Laine, BMC Syst. Biol. **2**, 74 (2008).

[11] M. Beran, Nuovo Cimento **38**, 771 (1965); S. Torquato and J. D. Beasley, Int. J. Eng. Sci. **24**, 415 (1986); S. Torquato and F. Lado, Proc. R. Soc. London, Ser. A **417**, 59 (1988); D. C. Pham and S. Torquato, J. Appl. Phys. **94**, 6591 (2003).

[12] M. J. Beran and J. Molyneux, Q. Appl. Math. **24**, 107 (1966); C. A. Miller and S. Torquato, J. Appl. Phys. **69**, 1948 (1991); J. Quintanilla and S. Torquato, *ibid.* **77**, 4361 (1995); S. Torquato, Phys. Rev. Lett. **79**, 681 (1997).

[13] S. Prager, Phys. Fluids **4**, 1477 (1961); J. D. Beasley and S. Torquato, Phys. Fluids A **1**, 199 (1989); S. Torquato and B. Lu, *ibid.* **2**, 487 (1990).

[14] S. Torquato and J. Rubinstein, J. Chem. Phys. **90**, 1644 (1989); S. Torquato and F. Lado, *ibid.* **94**, 4453 (1991); S. Torquato and D. C. Pham, Phys. Rev. Lett. **92**, 255505 (2004); D. C. Pham and S. Torquato, J. Appl. Phys. **97**, 013535 (2005).

[15] M. C. Rechtsman and S. Torquato, J. Appl. Phys. **103**, 084901 (2008).

[16] P. Debye and A. M. Bueche, J. Appl. Phys. **20**, 518 (1949).

[17] S. Torquato and G. Stell, J. Chem. Phys. **78**, 3262 (1983).

[18] S. Torquato, Soft Matter **5**, 1157 (2009).

[19] C. L. Y. Yeong and S. Torquato, Phys. Rev. E **57**, 495 (1998).

[20] C. L. Y. Yeong and S. Torquato, Phys. Rev. E **58**, 224 (1998).

[21] D. Cule and S. Torquato, J. Appl. Phys. **86**, 3428 (1999); N. Sheehan and S. Torquato, *ibid.* **89**, 53 (2001).

[22] M. G. Rozman and M. Utz, Phys. Rev. Lett. **89**, 135501 (2002); D. T. Fullwood, S. R. Niezgoda, B. L. Adams, and S. R. Kalidindi, Prog. Mater. Sci. **55**, 477 (2010).

[23] K. Wu, M. I. J. Dijke, G. D. Couples, Z. Jiang, J. Ma, K. S. Sorbie, J. Crawford, I. Young, and X. Zhang, Transp. Porous Media **65**, 443 (2006).

[24] M. A. Ansari and F. Stepanek, AlChE Journal **52**, 3762 (2006).

[25] R. Hilfer and C. Manwart, Phys. Rev. E **64**, 021304 (2001).

[26] D. Basanta, M. A. Miodownik, E. A. Holm, and P. J. Bentley, Metall. Mater. Trans. A **36**, 1643 (2005).

[27] H. Kumar, C. L. Briant, and W. A. Curtin, Mech. Mater. **38**, 818 (2006).

[28] Y. Jiao, F. H. Stillinger, and S. Torquato, Phys. Rev. E **76**, 031110 (2007).

[29] Y. Jiao, F. H. Stillinger, and S. Torquato, Phys. Rev. E **77**, 031135 (2008).

[30] D. T. Fullwood, S. R. Niezgoda, and S. R. Kalidindi, Acta Mater. **56**, 942 (2008).

[31] M. Boutin and G. Kemper, Adv. Appl. Math. **32**, 709 (2004).

[32] J. I. Yellott, Jr., J. Opt. Soc. Am. A **10**, 777 (1993).

[33] Y. Jiao, F. H. Stillinger, and S. Torquato, Proc. Natl. Acad. Sci. U.S.A. **106**, 17634 (2009).

[34] Y. Jiao, F. H. Stillinger, and S. Torquato, Phys. Rev. E **81**, 011105 (2010).

[35] S. Torquato, J. Chem. Phys. **85**, 4622 (1986); N. A. Seaton and E. D. Glandt, *ibid.* **85**, 5262 (1986); C. Vega, R. D. Kaminsky, and P. A. Monson, *ibid.* **99**, 3003 (1993).

[36] B. Lu and S. Torquato, Phys. Rev. A **45**, 922 (1992); **45**, 7292 (1992); D. Gueron and A. Mazzolo, Phys. Rev. E **68**, 066117 (2003); A. Mazzolo, J. Phys. A **37**, 7095 (2004).

[37] S. Torquato and B. Lu, Phys. Rev. E **47**, 2950 (1993).

[38] S. Torquato, J. D. Beasley, and Y. C. Chiew, J. Chem. Phys. **88**, 6540 (1988); S. B. Lee and S. Torquato, *ibid.* **91**, 1173 (1989).

[39] It is only for certain simple idealized textures that one can obtain a perfect match of the vector-argumented correlation functions associated with the reconstructed and target media [22].

[40] S. Torquato, J. Chem. Phys. **111**, 8832 (1999); Ind. Eng. Chem. Res. **45**, 6923 (2006); J. A. Quintanilla, Proc. R. Soc. London, Ser. A **464**, 1761 (2008).

[41] J. I. Yellott, Jr. and G. J. Iverson, J. Opt. Soc. Am. A **9**, 388 (1992).

[42] C. Chubb and J. I. Yellott, Vision Res. **40**, 485 (2000).

[43] S. Torquato and F. H. Stillinger, J. Appl. Phys. **102**, 093511 (2007); **103**, 129902 (2008).